Buckling of sandwich cylindrical shells with shear deformable core through nondimensional parameters

Uriol Balbin, I.; Bisagni, C.

DOI
10.1016/j.tws.2020.107393

Publication date
2021

Document Version
Final published version

Published in
Thin-Walled Structures

Thin–Walled Structures 161 (2021) 107393

Contents lists available at ScienceDirect

Thin-Walled Structures

journal homepage: http://www.elsevier.com/locate/tws

Buckling of sandwich cylindrical shells with shear deformable core through nondimensional parameters

Ines Uriol Balbin, Chiara Bisagni *

Delft University of Technology, Faculty of Aerospace Engineering, Delft, Netherlands

ARTICLE INFO

Keywords:
Analytical formulation
Nondimensionalisation
Transverse shear
Shell buckling

ABSTRACT

This paper presents the derivation of nondimensional buckling equations of sandwich cylindrical shells made of composite facesheets with a shear deformable core. The procedure yields an analytical solution in terms of a series of nondimensional parameters for the axial buckling load investigating the influence of the core transverse shear. The developed equations and the nondimensional parameters are used to study the buckling response of different shells, and the calculated buckling loads are compared to the buckling values obtained by neglecting the transverse shear. Graphs and tables are presented to show the effects of the nondimensional parameters on the nondimensional buckling load. The results are verified by finite element analyses using the commercial code Abaqus.

1. Introduction

Sandwich composite structures offer a large design space due to the diversity of materials available and the laminate constructions that are possible. Nondimensional parameters are particularly valuable to navigate this large design space [1]. For instance, many different constructions may correspond to the same set of nondimensional parameters, and the relative magnitudes of the parameters can be used to identify special cases in which one or more parameters are negligible. Nondimensional parameters also provide insight into the development of scaling technology used to reduce the cost of experimental validation and certification of large scale structures [2,3].

The earliest most well-known structural nondimensional parameter is the Batdorf parameter, introduced in 1940. It characterizes the impact of length, thickness and radius of curvature on the linear bifurcation buckling of isotropic cylinders [4]. In the 1990s, Nemeth developed nondimensional parameters and equations for linear bifurcation buckling of symmetrically laminated shallow shells with double curvature [5]. From 2002 to 2008, Weaver et al. [6] made extensive use of nondimensionalisation procedures and parameters to gain insight into the behavior of laminated composite structures. In their study, to account for the effects of flexural-twist and extension-twist anisotropies on the buckling of compression loaded cylindrical shells, correction factors derived from the nondimensionalisation procedures were calculated. In the field of the buckling of sandwich composite structures with shear deformable core, nondimensional parameters have been used to study and characterize plates [7].

Understanding the structural behavior of sandwich composite cylindrical shells is important in modern, high-performance applications, where they are a fundamental component of many lightweight structures, such as aircraft and spacecraft. One particular area of interest is the shell buckling strength under compression loads. Due to the nonlinearity of the phenomenon and the high dependence on imperfections, robust design criteria must be developed [8]. Therefore, axially loaded cylindrical shells have been investigated through testing, simulation and analysis.

Testing is an invaluable resource in the study of buckling of sandwich composite cylindrical shells, since it provides validation of numerical and analytical methods [9] used by designers. Knock-down factors (KDF), which are still widely used to account for imperfections in the axial buckling of shells, were obtained via extensive testing [10]. However, testing is expensive, due not only to the high number of test required but also due to the large scale of the structures considered [11]. Moreover, the test data are highly dependent on the manufacturing characteristics and imperfection signature of the shell [12].

Simulation tools used to predict the buckling of sandwich composite cylindrical shells have also been thoroughly investigated [13]. One of the advantages is that they allow for greater detail in the design features such as the inclusion of cut-outs [14]. Continuum shell elements [15] as well as conventional shell formulation [16] have proven valuable to

* Corresponding author.
E-mail address: c.bisagni@tudelft.nl (C. Bisagni).

https://doi.org/10.1016/j.tws.2020.107393
Received 25 June 2020; Received in revised form 7 November 2020; Accepted 18 December 2020
Available online 15 January 2021

study the influence of transverse shear in the buckling of shells. Simulations are able to produce accurate results as long as the precise dimensions and imperfection signature are available [17].

Despite tests and numerical simulations importance, analytical models are the first tool designers use in order to predict the buckling behavior of the structure. Analytical calculations are faster and more flexible to dimension and/or material changes [18]. However, making the right assumptions and choosing the appropriate analytical model is a prerequisite to getting accurate results. One challenge of modeling sandwich composite shells is the inclusion of the shear deformable core. Several models for laminate plates and shells that include the transverse shear are available in the literature [19]. These modeling approaches can be divided in categories depending upon the variation of the displacement components through the thickness.

Most analytical modeling approaches are based on a first order shear deformation theory [20,21], where a cross section, normal to the mid-surface of the undeformed state, remains flat but not normal in the deformed state. A correction factor has to be used to adjust the transverse shear stiffness. Other models are based on a higher order theory [22]. Higher order, in this case, does not refer to the order of the final system of differential equations but to the number of terms in the power series expansion of the displacements. Higher order theories account for shear rotations and parabolic variation of the shear stresses, which have the advantage of eliminating the need for shear correction factors [23]. Finally, other authors have proposed more complex formulations such as incorporating the first-order shear deformation theory kinematics with zig-zag layer functions [24] or a sublaminate formulation [25].

This study aims to extend existing nondimensionalisation work to sandwich composite cylindrical shells with shear deformable core under axial compression. The facesheets are modeled using the two-dimensional classical laminate theory based on the Kirchhoff-Love assumptions. This approach was used in the Nemeth formulation [26] and it is considered sufficiently accurate. The shear-deformable core is modeled including in the equations a transverse shear deformation theory.

To obtain the axial nondimensional buckling load, first the problem and its assumptions are described. This includes the geometry and properties of the shell, as well as the nondimensional reference system and nondimensional displacements. Then, the fundamental relations are explained and derived both in the dimensional and nondimensional form: strain-displacement relations, constitutive equations, equilibrium equations and compatibility equations. The equilibrium and compatibility equations are linearized, possible solutions according to the boundary conditions are proposed and the eigenvalue problem resultant is solved for the buckling load. Finally, some applications of the methodology are shown in order to illustrate the advantages of using the nondimensional parameters, and to explore the full design space that sandwich composite shells can offer.

2. Nondimensional formulation

Sandwich composite structures provide bending and in-plane extensional rigidity with composite facesheets separated by a low density core, which provides as well transverse shear rigidity to the construction. The laminated sandwich shells under consideration are composed of identical inner and outer facesheets and a core made of a shear deformable material. The facesheets are made of several laminae whose fibers can be oriented in any direction and any stacking sequence of the laminae is permissible.

The geometry of the shell is characterized by its length L, radius of the middle surface R, facesheet thickness t_f, and core thickness t_c as depicted in Fig. 1 and Fig. Geo. Consistent with the shells formulation, the assumption that the shell thickness is small compared to the radius is made. The mid-surface of the sandwich construction is the reference surface. The distance between the mid-surfaces of the inner and outer facesheets, h, is also defined.

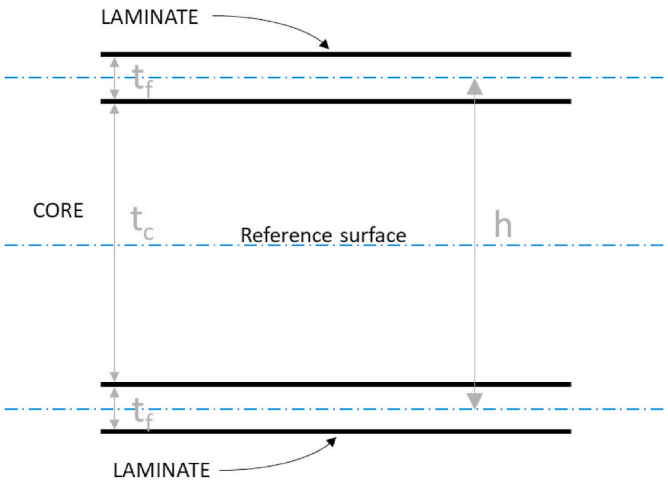

Fig. 1. Shell section.

In this study, both facesheets are assumed to have an equal thickness and they are placed symmetric with respect to the mid-surface of the sandwich construction. Therefore, the entire sandwich is symmetric even if the layup of the facesheets is not. Each ply in both facesheets is orthotropic, linear elastic, and of constant thickness, whereupon the entire shell is of constant thickness. Facesheets are sufficiently thin (as compared to the core) so that their transverse shear properties won't be taken into account. The core is orthotropic, with one axis of orthotropy parallel to the axis of the shell, linear elastic and of constant thickness.

The coordinate system x, y, z is measured with respect to the reference surface in the axial, circumferential and radial directions respectively as depicted in Fig. 2. The nondimensional or normalized coordinates, z_1, z_2 and z_3 are:

$$z_1 = \frac{x}{L} \tag{1}$$

$$z_2 = \frac{y}{R} \tag{2}$$

$$z_3 = \frac{z}{\sqrt{12}\sqrt[4]{a_{11}a_{22}D_{11}D_{22}}} \tag{3}$$

where the a_{ii} are membrane compliance's and the D_{ii} are bending stiffness's of the entire sandwich and are calculated using the classical laminate theory.

The denominator $\sqrt{12}\sqrt[4]{a_{11}a_{22}D_{11}D_{22}}$ of Eq. (3) represents the

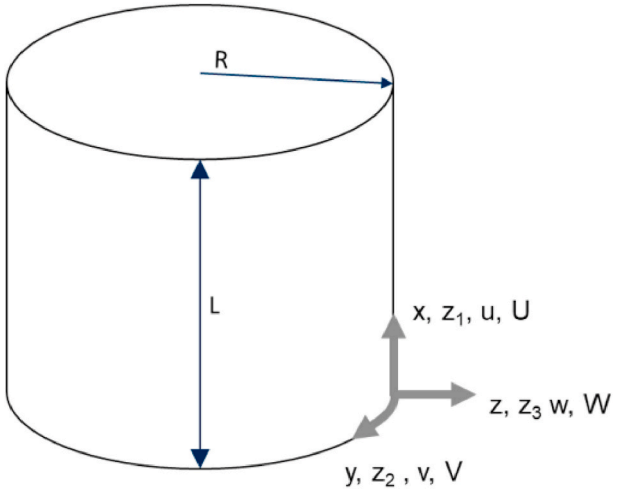

Fig. 2. Cylindrical shell geometry and coordinate system.

equivalent thickness of the sandwich structure. In the particular case where the structure is made of an isotropic material instead of a sandwich composite, the value of the equivalent thickness is the value of the exact thickness.

The components of displacement u, v and w of a point on the shell are the components in the x, y and z directions. The nondimensional displacements U, V, W are defined as:

$$U = \frac{L}{\sqrt{a_{11}a_{22}D_{11}D_{22}}}\, u \tag{4}$$

$$V = \frac{R}{\sqrt{a_{11}a_{22}D_{11}D_{22}}}\, v \tag{5}$$

$$W = \frac{1}{\sqrt[4]{a_{11}a_{22}D_{11}D_{22}}}\, w \tag{6}$$

The transverse shear rigidity is provided mainly by the core, so only the transverse shear properties of the core will be included in the formulation. The transverse shear stresses are also assumed constant through the thickness of the core. With this assumption, a modeling approach based on the first order shear deformation theory of Cheung and Tennyson [27] is proposed. The transverse shear stress distribution across the sandwich wall is assumed to satisfy the continuity requirement at the interfaces between the facesheet and the core, and vanishes on the free surfaces. As a result, a linear distribution of the in-plane displacement components of the core is obtained through the thickness. In the shear deformation theory of Cheung and Tennyson, no shear correction factor is explicitly included. The model considers that a correction factor is included by establishing the distance h described in Fig. 1, instead of exclusively the core thickness.

The shell is considered to have simply supported boundary conditions. Some assumptions are made in order to proceed with the analysis. First, no failure between the facesheet and the core is assumed. In the laminate there is no slippage between plies, as well as no intercell buckling in the core. Finally, the normal stiffness of the core is considered very large, therefore instability associated with wrinkling of facesheets is not included.

The process to obtain the buckling load and mode of the shell follows the classical procedure [28]. First, the strains-displacement relations are established according to the proposed assumptions. Secondly, the equilibrium and compatibility equations are developed step by step and transformed into the nondimensional formulation. In order to obtain these equations, the strains-displacement relations are adapted to nondimensional form. The nondimensional linear buckling equations are obtained applying the adjacent equilibrium criterion [29] and a nondimensional axial buckling load solution is presented for the formulation with and without core transverse shear.

3. Equilibrium and compatibility equations

The equations used in the present study are relatively well known in their dimensional form [28]. The current nondimensionalisation keeps a similar format as the dimensional equations and it is here applied to axial compression. The formulation also can be used for other load cases.

First, the displacement field distribution and the strain displacement relations are presented. Then, the stress resultants and constitute equations are considered and the nonlinear equilibrium equations and the strain compatibility equation are obtained.

3.1. Strain-displacement relations

Using the nonlinear strain-displacement relations, where strains are small, strains components ε_x, ε_y, γ_{xy}, γ_{xz} and γ_{yz} can be expressed as:

$$\varepsilon_x = \varepsilon_x^0 - z\frac{\partial \beta_x}{\partial x} = \frac{\partial u}{\partial x} + \frac{1}{2}\left(\frac{\partial w}{\partial x}\right)^2 - z\frac{\partial \beta_x}{\partial x} \tag{7}$$

$$\varepsilon_y = \varepsilon_y^0 - z\frac{\partial \beta_y}{\partial y} = \frac{\partial v}{\partial y} + \frac{w}{R} + \frac{1}{2}\left(\frac{\partial w}{\partial y}\right)^2 - z\frac{\partial \beta_y}{\partial y} \tag{8}$$

$$\gamma_{xy} = \gamma_{xy}^0 - z\left(\frac{\partial \beta_y}{\partial y} + \frac{\partial \beta_x}{\partial y}\right) = \frac{\partial v}{\partial x} + \frac{\partial u}{\partial y} + \frac{\partial w}{\partial x}\frac{\partial w}{\partial y} - z\left(\frac{\partial \beta_y}{\partial x} + \frac{\partial \beta_x}{\partial y}\right) \tag{9}$$

$$\gamma_{xz} = \left(\frac{\partial w}{\partial y} - \beta_y\right) \tag{10}$$

$$\gamma_{yz} = \left(\frac{\partial w}{\partial x} - \beta_x\right) \tag{11}$$

where ε_y^0, ε_y^0 and γ_{xy}^0 are the components of the strains at the reference surface and β_x and β_y are the components of the change of slope of the normal to the undeformed mid-surface.

These components, β_x and β_y, are already nondimensional and could be kept as is, in their classical form. However, the equations simplify considerably if two new normalized parameters, B_1 and B_2, are established:

$$B_1 = \frac{L}{\sqrt[4]{a_{11}a_{22}D_{11}D_{22}}}\, \beta_x \tag{12}$$

$$B_2 = \frac{R}{\sqrt[4]{a_{11}a_{22}D_{11}D_{22}}}\, \beta_y \tag{13}$$

The strain equations ((Eqs. (7)–(11)) can be also defined in terms of the nondimensional coordinates and displacements (Eqs. (1)–(6), (12) and (13)), where the nondimensional strains, E_{11}, E_{22}, Γ_{12}, Γ_{13} and Γ_{23} are expressed as:

$$E_{11} = \frac{L^2}{\sqrt{a_{11}a_{22}D_{11}D_{22}}}\, \epsilon_x = \frac{\partial U}{\partial z_1} + \frac{1}{2}\left(\frac{\partial W}{\partial z_1}\right)^2 - z_3\frac{\partial B_1}{\partial z_1} \tag{14}$$

$$E_{22} = \frac{R^2\, \varepsilon_y}{\sqrt{a_{11}a_{22}D_{11}D_{22}}} = \frac{\partial V}{\partial z_2} + \frac{R}{\sqrt[4]{a_{11}a_{22}D_{11}D_{22}}}W + \frac{1}{2}\left(\frac{\partial W}{\partial z_2}\right)^2 - z_3\frac{\partial B_1}{\partial z_2} \tag{15}$$

$$\Gamma_{12} = \frac{LR}{\sqrt{a_{11}a_{22}D_{11}D_{22}}}\, \gamma_{xy} = \frac{\partial V}{\partial z_1} + \frac{\partial U}{\partial z_2} + \frac{\partial W}{\partial z_1}\frac{\partial W}{\partial z_2} - z_3\left(\frac{\partial B_2}{\partial z_1} + \frac{\partial B_1}{\partial z_2}\right) \tag{16}$$

$$\Gamma_{13} = \frac{R^2}{\sqrt{a_{11}a_{22}D_{11}D_{22}}}\, \gamma_{xz} = \frac{\partial W}{\partial z_2} - B_2 \tag{17}$$

$$\Gamma_{23} = \frac{L^2}{\sqrt{a_{11}a_{22}D_{11}D_{22}}}\, \gamma_{yz} = \frac{\partial W}{\partial z_1} - B_1 \tag{18}$$

Due to the chosen nondimensionalisation procedure, most the equations in their nondimensional format (Eqs. (10), (14), (16) and (18)) only include the derivations of nondimensional displacements U,V, W and the components of the change of slope of the normal B_1, B_2 with respect to the introduced nondimensional coordinates z_1, z_2.

However, in Eq. (15), there is also the term: $R/\sqrt[4]{a_{11}a_{22}D_{11}D_{22}}$. With few modifications this term can be expressed as Z, a nondimensional parameter known as the Batdorf-Stein parameter.

$$Z = \frac{R}{\sqrt{12}\sqrt[4]{a_{11}a_{22}D_{11}D_{22}}} \tag{19}$$

The Batdorf-Stein parameter, Z, formally introduced by Nemeth [5], relates the radius with the membrane compliances and bending stiffnesses. The Batdorf-Stein parameter is similar in character to a radius to thickness ratio (R/t) because it relates the shell radius (R) to an equivalent thickness ($\sqrt{12}\sqrt[4]{a_{11}a_{22}D_{11}D_{22}}$).

Eq. (15) results then as:

$$E_{22} = \frac{\partial V}{\partial z_2} + \sqrt{12}\, Z\, W + \frac{1}{2}\left(\frac{\partial W}{\partial z_2}\right)^2 - z_3\frac{\partial B_1}{\partial z_2} \tag{20}$$

From Eqs. (14), (16) and (20), the nondimensional expressions of the reference surface strains can be obtained:

$$E_{11}^0 = \frac{\partial U}{\partial z_1} + \frac{1}{2}\left(\frac{\partial W}{\partial z_1}\right)^2 \tag{21}$$

$$E_{22}^0 = \frac{\partial V}{\partial z_2} + \sqrt{12}\, Z\, W + \frac{1}{2}\left(\frac{\partial W}{\partial z_2}\right)^2 \tag{22}$$

$$\Gamma_{12}^0 = \frac{\partial V}{\partial z_1} + \frac{\partial U}{\partial z_2} + \frac{\partial W}{\partial z_1}\frac{\partial W}{\partial z_2} \tag{23}$$

In a similar way as the strains at any point of the shell are described in Eqs. (14), (16) and (20), the nondimensional values of the mid-surface strains E_{11}, E_{22} and Γ_{12} are thus expressed as:

$$E_{11}^0 = \frac{L^2}{\sqrt{a_{11}a_{22}D_{11}D_{22}}}\,\varepsilon_x^0 \tag{24}$$

$$E_{22}^0 = \frac{R^2}{\sqrt{a_{11}a_{22}D_{11}D_{22}}}\,\varepsilon_y^0 \tag{25}$$

$$\Gamma_{12}^0 = \frac{LR}{\sqrt{a_{11}a_{22}D_{11}D_{22}}}\,\gamma_{xy}^0 \tag{26}$$

3.2. Constitutive equations

In deriving a set of nondimensional constitutive equations, it is desirable to keep the number of parameters that characterize the material behavior to a minimum. Here, the semi-inverted constitutive equations are used, considering that the sandwich structure is symmetric, even if the laminates that conform the facesheets are not.

$$\varepsilon_x^0 = a_{11}N_x + a_{12}N_y \tag{27}$$

$$\varepsilon_y^0 = a_{12}N_x + a_{22}N_y \tag{28}$$

$$\gamma_{xy}^0 = a_{66}N_{xy} \tag{29}$$

where N_x, N_y and N_{xy} are the force components per unit length. The nondimensional components of these forces: $\mathcal{N}_{11}$, $\mathcal{N}_{22}$ and $\mathcal{N}_{12}$, can be defined as:

$$\mathcal{N}_{11} = \frac{R^2}{\sqrt{D_{11}D_{22}}}N_x \tag{30}$$

$$\mathcal{N}_{22} = \frac{L^2}{\sqrt{D_{11}D_{22}}}N_y \tag{31}$$

$$\mathcal{N}_{12} = \frac{R^2}{\sqrt[4]{D_{11}D_{22}^3}}N_{xy} \tag{32}$$

Combining the in-plane equations (Eqs. (27) and (28)) with the definitions of the nondimensional strains (Eqs. (24) and (25)) and nondimensional stresses (Eqs. (30) and (31)) and operating, the following nondimensional in-plane relations are obtained:

$$E_{11}^0 = \frac{L^2}{R^2}\sqrt[2]{\frac{a_{11}}{a_{22}}}\mathcal{N}_{11} + \frac{a_{12}}{\sqrt{a_{11}a_{22}}}\mathcal{N}_{22} \tag{33}$$

$$E_{22}^0 = \frac{a_{12}}{\sqrt{a_{11}a_{22}}}\mathcal{N}_{11} + \frac{R^2}{L^2}\sqrt[2]{\frac{a_{22}}{a_{11}}}\mathcal{N}_{22} \tag{34}$$

In these two equations, three new terms appear. Upon inspection, these three terms can be expressed with the help of two nondimensional parameters α_m and ν_m, as defined by Nemeth [5]:

$$\alpha_m = \frac{R}{L}\sqrt[4]{\frac{a_{22}}{a_{11}}} \tag{35}$$

$$\nu_m = -\frac{a_{12}}{\sqrt{a_{11}a_{22}}} \tag{36}$$

Combining the in-plane shear equation (Eq. (29)) with the definition of the nondimensional strain (Eq. (26)) and nondimensional in-plane shear stress (Eq. (32)) and operating, the following relation is obtained:

$$\Gamma_{12}^0 = \frac{L}{R}\frac{a_{66}}{\sqrt{a_{11}a_{22}}}\sqrt[2]{\frac{D_{22}}{D_{11}}}\mathcal{N}_{12} \tag{37}$$

Operating it can become:

$$\Gamma_{12}^0 = \frac{L}{R}\sqrt[2]{\frac{D_{22}}{D_{11}}}2\left(\frac{2a_{12}+a_{66}}{2\sqrt{a_{11}a_{22}}} - \frac{a_{12}}{\sqrt{a_{11}a_{22}}}\right)\mathcal{N}_{12} \tag{38}$$

This equation can be expressed with the help of three nondimensional parameters as defined by Nemeth [5]: ν_m (already been defined in Eq. (36)), α_b, and μ:

$$\alpha_b = \frac{R}{L}\sqrt[4]{\frac{D_{11}}{D_{22}}} \tag{39}$$

$$\mu = \frac{2a_{12}+a_{66}}{2\sqrt{a_{11}a_{22}}} \tag{40}$$

The parameters α_m (Eq. (35)) and α_b (Eq. (39)) are called the stiffness weighted geometry parameters, because they relate the geometry of the shell: radius and length, with the stiffness of the composite laminate. The membrane orthotropy parameter, μ (Eq. (40)) and membrane Poisson ratio, ν_m (Eq. (36)) relate to the membrane compliance and are mostly dependent on the material properties and facesheet layup.

If the nondimensional parameters (Eqs. (35), (36), (39) and (40)) are included in the in-plane relations (Eqs. (33), (34) and (38)) a more compact formulation can be expressed:

$$\begin{bmatrix} E_{11}^0 \\ E_{22}^0 \\ \Gamma_{12}^0 \end{bmatrix} = \begin{bmatrix} \frac{1}{\alpha_m^2} & -\nu_m & 0 \\ -\nu_m & \alpha_m^2 & 0 \\ 0 & 0 & \frac{2(\mu+\nu_m)}{\alpha_b} \end{bmatrix} \begin{bmatrix} \mathcal{N}_{11} \\ \mathcal{N}_{22} \\ \mathcal{N}_{12} \end{bmatrix} \tag{41}$$

Under the current assumptions, the bend-twist anisotropy is treated as negligible. This means that even if the value is not zero the influence of the bend-twist terms compared to other bending terms is considered small. This assumption might not be valid for all laminates especially for cases where the facesheets have a low ply number. Under this assumption, the moment per unit length resultants are defined as:

$$M_x = -\left(D_{11}\frac{\partial \beta_x}{\partial x} + D_{12}\frac{\partial \beta_y}{\partial y}\right) \tag{42}$$

$$M_y = -\left(D_{12}\frac{\partial \beta_x}{\partial x} + D_{22}\frac{\partial \beta_y}{\partial y}\right) \tag{43}$$

$$M_{xy} = -D_{66}\left(\frac{\partial \beta_y}{\partial x} + \frac{\partial \beta_x}{\partial y}\right) \tag{44}$$

In a similar way to the nondimensional force resultants described in Eqs. (30)–(32), the nondimensional moment resultants are introduced as follows:

$$\mathcal{M}_{11} = \frac{R^2}{\sqrt[4]{a_{11}a_{22}D_{11}^3D_{22}^3}}M_x \tag{45}$$

$$\mathcal{M}_{22} = \frac{L^2}{\sqrt[4]{a_{11}a_{22}D_{11}^3D_{22}^3}}M_y \tag{46}$$

$$\mathcal{M}_{12} = \frac{RL}{\sqrt[4]{a_{11}a_{22}D_{11}^3D_{22}^3}}M_{xy} \tag{47}$$

Combining the moment equations (Eqs. (42) and (43)) with the definitions of the nondimensional change of slope to the normal of the undeformed mid-surface (Eqs. (12) and (13)) and nondimensional moments (Eqs. (45)–47)) the following relations are obtained:

$$\mathscr{M}_{11} = -\frac{R^2}{L^2}\sqrt[2]{\frac{D_{11}}{D_{22}}}\frac{\partial B_1}{\partial z_1} - \frac{D_{12}}{\sqrt{D_{11}D_{22}}}\frac{\partial B_2}{\partial z_2} \tag{48}$$

$$\mathscr{M}_{22} = -\frac{R^2}{L^2}\sqrt[2]{\frac{D_{11}}{D_{22}}}\frac{\partial B_2}{\partial z_2} - \frac{D_{12}}{\sqrt{D_{11}D_{22}}}\frac{\partial B_1}{\partial z_1} \tag{49}$$

In these relations, two terms appear that can be expressed through the nondimensional parameters α_b and ν_b as introduced by Nemeth [5]. The parameter α_b, used in the in-plane relations, is already defined (Eq. (39)) and the parameter ν_b is expressed as:

$$\nu_b = \frac{D_{12}}{\sqrt{D_{11}D_{22}}} \tag{50}$$

The nondimensional parameter, ν_b, similarly to ν_m from Eq. (36), is called the flexural Poisson ratio and relates the bending stiffness terms of the sandwich composite.

If the moment equation Eq. (44) and the expression of nondimensional moment Eq. (47) is taken in combination with the definitions of the nondimensional change of slope to the normal of the undeformed mid-surface (Eqs. (12) and (13)), the following relation is obtained:

$$\mathscr{M}_{12} = -\frac{D_{66}}{\sqrt[4]{D_{11}D_{22}}}\left(\frac{\partial B_2}{\partial z_1} + \frac{\partial B_1}{\partial z_2}\right) \tag{51}$$

Manipulating this equation, it can be obtained that it is equivalent to:

$$\mathscr{M}_{12} = -\frac{1}{2}\left(\frac{D_{12}+2D_{66}}{\sqrt{D_{11}D_{22}}} + \frac{D_{12}}{\sqrt{D_{11}D_{22}}}\right)\left(\frac{\partial B_2}{\partial z_1} + \frac{\partial B_1}{\partial z_2}\right) \tag{52}$$

In this expression, two parameters can be extracted. On the one hand, the flexural Poisson ratio, ν_b described in Eq. (50). On the other hand, the flexural orthotropy parameter, β, defined as:

$$\beta = \frac{D_{12}+2D_{66}}{\sqrt{D_{11}D_{22}}} \tag{53}$$

The flexural orthotropy parameter β is analogous to the membrane orthotropy parameter μ (Eq. (40). It describes the interaction between the terms of the bending stiffness matrix and as such is highly dependent on the facesheet layup and material properties. The dependence on the core thickness is low because it affects similarly the terms on the numerator and denominator. This is particularly valuable to study separately the influence of the thickness and the influence of the material properties.

If the nondimensional parameters are included in the moment expressions (Eqs. (48), (49) and (52)) the result is:

$$\begin{bmatrix}\mathscr{M}_{11}\\ \mathscr{M}_{22}\\ \mathscr{M}_{12}\end{bmatrix} = -\begin{bmatrix}\alpha_b^2 & \nu_b & 0\\ \nu_b & \frac{1}{\alpha_b^2} & 0\\ 0 & 0 & \frac{(\beta-\nu_b)}{2}\end{bmatrix}\begin{bmatrix}\frac{\partial B_1}{\partial z_1}\\ \frac{\partial B_2}{\partial z_2}\\ \frac{\partial B_2}{\partial z_1}+\frac{\partial B_1}{\partial z_2}\end{bmatrix} \tag{54}$$

Finally, the transverse shear stress resultants Q_x and Q_y can be expressed under the current model assumptions as:

$$Q_x = G_x h\left(\frac{\partial w}{\partial x} - \beta_x\right) \tag{55}$$

$$Q_y = G_y h\left(\frac{\partial w}{\partial y} - \beta_y\right) \tag{56}$$

In the nondimensional form, following a similar procedure as with the force and moment resultants, the transverse shear force resultants $\mathscr{Q}_{11}$ and $\mathscr{Q}_{22}$ are defined as:

$$\mathscr{Q}_{11} = \frac{LR^2}{\sqrt[4]{a_{11}a_{22}D_{11}^3D_{22}^3}}Q_x \tag{57}$$

$$\mathscr{Q}_{22} = \frac{L^2R}{\sqrt[4]{a_{11}a_{22}D_{11}^3D_{22}^3}}Q_y \tag{58}$$

Combining the transverse shear force resultant definition (Eqs. (55) to (58)) and the slope components (Eqs. (12) and (13)), the corresponding constitutive equations for the transverse shear force resultants in nondimensional form are obtained:

$$\mathscr{Q}_{11} = \frac{G_x hR^2}{\sqrt{D_{11}D_{22}}}\left(\frac{\partial W}{\partial z_1} - B_1\right) \tag{59}$$

$$\mathscr{Q}_{22} = \frac{G_y hL^2}{\sqrt{D_{11}D_{22}}}\left(\frac{\partial W}{\partial z_2} - B_2\right) \tag{60}$$

From these expressions, two clear terms emerge and thus two new nondimensional parameters can be defined as:

$$\chi_1 = \frac{G_x hR^2}{\sqrt{D_{11}D_{22}}} \tag{61}$$

$$\chi_2 = \frac{G_y hL^2}{\sqrt{D_{11}D_{22}}} \tag{62}$$

The nondimensional parameters χ_1 and χ_2 were not part of the nondimensionalisation proposed by Nemeth [5]. The objective of the two new nondimensional parameters is to represent the influence of the core shear properties with respect to the sandwich bending stiffness and the geometry properties of the shell. The influence of these parameters will give an indication of the importance of the transverse shear in the buckling loads of the shell.

Instead of considering χ_1 and χ_2 separately, a transverse ratio (φ) is defined:

$$\varphi = \frac{\chi_2}{\chi_1} = \frac{G_y}{G_x}\left(\frac{L}{R}\right)^2 \tag{63}$$

This is a more convenient way of studying the problem since the properties of the core G_x and G_y are not independent from each other and must be considered together. The parameter φ also presents an advantage for cases with isotropic core materials, where the transverse ratio (φ) depends only on the geometry of the shell, as $G_x = G_y$.

With the inclusion of χ_1 and χ_2 the transverse shear force resultants are:

$$\begin{bmatrix}\mathscr{Q}_{11}\\ \mathscr{Q}_{22}\end{bmatrix} = \begin{bmatrix}\chi_1 & 0\\ 0 & \varphi\chi_1\end{bmatrix}\begin{bmatrix}\frac{\partial W}{\partial z_1} - B_1\\ \frac{\partial W}{\partial z_2} - B_2\end{bmatrix} \tag{64}$$

3.3. Equilibrium equations

Assuming the transverse normal stiffness of the sandwich shell as infinite, and considering the nondimensional formulation presented, the nondimensional equilibrium equations of forces and moments for a thin cylindrical shell are:

$$\frac{\partial \mathscr{N}_{11}}{\partial z_1} + \frac{1}{\alpha_b}\frac{\partial \mathscr{N}_{12}}{\partial z_2} = 0 \tag{65}$$

$$\frac{1}{\alpha_b}\frac{\partial \mathscr{N}_{12}}{\partial z_1} + \frac{\partial \mathscr{N}_{22}}{\partial z_2} = 0 \tag{66}$$

$$\frac{\partial \mathscr{Q}_1}{\partial z_1} + \frac{\partial \mathscr{Q}_2}{\partial z_2} + \mathscr{N}_{11}\frac{\partial^2 W}{\partial z_1^2} + \frac{2}{\alpha_b}\mathscr{N}_{12}\frac{\partial^2 W}{\partial z_1 \partial z_2} + \mathscr{N}_{22}\left(\frac{\partial^2 W}{\partial z_2^2} - \sqrt{12}Z\right) = 0 \tag{67}$$

$$\mathscr{C}_{11} = \frac{\partial \mathscr{M}_{11}}{\partial z_1} + \frac{\partial \mathscr{M}_{12}}{\partial z_2} \tag{68}$$

$$\mathscr{C}_{22} = \frac{\partial \mathscr{M}_{22}}{\partial z_2} + \frac{\partial \mathscr{M}_{12}}{\partial z_1} \tag{69}$$

The first two equations of equilibrium (Eqs. (65) and (66)) are satisfied introducing the stress function $F(z_1 z_2)$ defined as:

$$\mathscr{N}_{11} = \frac{\partial^2 F}{\partial z_2^2} \tag{70}$$

$$\mathscr{N}_{22} = \frac{\partial^2 F}{\partial z_1^2} \tag{71}$$

$$\frac{\mathscr{N}_{12}}{\alpha_b} = -\frac{\partial^2 F}{\partial z_1 \partial z_2} \tag{72}$$

If equilibrium equations as expressed via the stress function F in Eqs. (70)–(72) are substituted in the third equilibrium equation Eq. (67), it yields:

$$\begin{aligned} &\frac{\partial^2 \mathscr{M}_{11}}{\partial z_1^2} + 2\frac{\partial^2 \mathscr{M}_{12}}{\partial z_1 \partial z_1} + \frac{\partial^2 \mathscr{M}_{22}}{\partial z_2^2} \\ &+\frac{\partial^2 F}{\partial z_2^2}\frac{\partial^2 W}{\partial z_1^2} - 2\frac{\partial^2 F}{\partial z_1 \partial z_2}\frac{\partial^2 W}{\partial z_1 \partial z_2} + \frac{\partial^2 F}{\partial z_1^2}\left(\frac{\partial^2 W}{\partial z_2^2} - \sqrt{12}Z\right) = 0 \end{aligned} \tag{73}$$

If the moment expressions as defined in Eqs. (45)–(47) are introduced in Eq. (73), it yields:

$$\begin{aligned} &-\alpha_b^2\frac{\partial^3 B_1}{\partial z_1^3} - \beta\frac{\partial^3 B_1}{\partial z_1 \partial z_2^2} - \frac{1}{\alpha_b^2}\frac{\partial^3 B_2}{\partial z_2^3} - \beta\frac{\partial^3 B_1}{\partial z_1^2 \partial z_2} \\ &= -\frac{\partial^2 F}{\partial z_2^2}\frac{\partial^2 W}{\partial z_1^2} + 2\frac{\partial^2 F}{\partial z_1 \partial z_2}\frac{\partial^2 W}{\partial z_1 \partial z_2} - \frac{\partial^2 F}{\partial z_1^2}\left(\frac{\partial^2 W}{\partial z_2^2} - \sqrt{12}Z\right) \end{aligned} \tag{74}$$

Finally, if the moment expressions Eq. (54) and the transverse force expressions Eq. (64) are used in the moment equilibrium equations (Eqs. (68) and (69)), the following relations are obtained:

$$\chi_1 B_1 - \alpha_b^2\frac{\partial^2 B_1}{\partial z_1^2} + \frac{1}{2}(\beta - \nu_b)\frac{\partial^2 B_1}{\partial z_2^2} - \frac{1}{2}(\beta + \nu_b)\frac{\partial^2 B_2}{\partial z_1 \partial z_2} = \chi_1\frac{\partial W}{\partial z_1} \tag{75}$$

$$\chi_2 B_2 - \frac{1}{\alpha_b^2}\frac{\partial^2 B_2}{\partial z_2^2} + \frac{1}{2}(\beta - \nu_b)\frac{\partial^2 B_2}{\partial z_1^2} - \frac{1}{2}(\beta + \nu_b)\frac{\partial^2 B_1}{\partial z_1 \partial z_2} = \chi_2\frac{\partial W}{\partial z_2} \tag{76}$$

3.4. Compatibility equations

The compatibility equation places restrictions on how the strains can vary over the shell so that a continuous displacement field could be found for the assumed strain field. The out of plane displacement, w in terms of the mid-surface strains: ε_x^0, ε_y^0 and γ_{xy}^0 is:

$$\frac{\partial^2 \varepsilon_x^0}{\partial y^2} + \frac{\partial^2 \varepsilon_y^0}{\partial x^2} - \frac{\partial^2 \gamma_{xy}^0}{\partial x y} = \frac{1}{R}\frac{\partial^2 w}{\partial x^2} + \left(\frac{\partial^2 w}{\partial y^2}\right)^2 - \frac{\partial^2 w}{\partial x^2}\frac{\partial^2 w}{\partial y^2} \tag{77}$$

Introducing the nondimensional mid-surface strains as described in (Eqs. (21)–(23), the derivatives of the nondimensional out-of-plane displacement as defined in Eq. (6), and the Batdorf-Stein parameter from Eq. (19), Eq. (77) is converted into the following nondimensional compatibility equation.

$$\frac{\partial^2 E_{11}^0}{\partial z_2^2} + \frac{\partial^2 E_{22}^0}{\partial z_1^2} - \frac{\partial^2 \Gamma_{12}^0}{\partial z_1 z_2} = \sqrt{12}Z\frac{\partial^2 W}{\partial z_1^2} + \frac{L^2}{R^2}\left(\frac{\partial^2 W}{\partial z_2^2}\right)^2 - \frac{\partial^2 W}{\partial z_1^2}\frac{\partial^2 W}{\partial z_2^2} \tag{78}$$

Introducing the constitutive equations Eq. (41) and the described stress function F (Eqs. (70)–(72)) the nondimensional compatibility equation becomes:

$$\alpha_m^2\frac{\partial^4 F}{\partial z_1^4} + \frac{1}{\alpha_m^2}\frac{\partial^4 F}{\partial z_2^4} + 2\mu\frac{\partial^4 F}{\partial z_1^2 \partial z_2^2} = \sqrt{12}Z\frac{\partial^2 W}{\partial z_1^2} + \frac{L^2}{R^2}\left(\frac{\partial^2 W}{\partial z_2^2}\right)^2 - \frac{\partial^2 W}{\partial z_1^2}\frac{\partial^2 W}{\partial z_2^2} \tag{79}$$

4. Linearized buckling equations taking into account transverse shear

The linearized equations for the determination of the critical buckling load at the bifurcation point can be derived by the application of the adjacent equilibrium criterion [29]. To investigate the existence of adjacent equilibrium configurations, it is assumed that the following variables W, F, B_1 and B_2 are given by:

$$W = \overline{W} + \widehat{W} \tag{80}$$

$$F = \overline{F} + \widehat{F} \tag{81}$$

$$B_1 = \overline{B_1} + \widehat{B}_1 \tag{82}$$

$$B_2 = \overline{B_2} + \widehat{B}_2 \tag{83}$$

where $\overline{W}$, $\overline{F}$, $\overline{B_1}$ and $\overline{B_2}$ represent the prebuckling solutions along the fundamental path and $\widehat{W}$, $\widehat{F}$ represent small perturbations at buckling. Assuming the shell is sufficiently long, the prebuckling displacement $\overline{W}$ and the prebuckling slope $\overline{B_1}$ and $\overline{B_2}$ are considered constant. This means that previous to the buckling event, both the out-of-plane displacement and the slopes are independent of the spatial coordinates z_1 and z_2.

The scope of this study is limited to shells under only axial compression to investigate the influence of the transverse shear in the axial buckling load, P. However, the nondimensionalisation until here can be utilized for other load cases. The equations are to be solved for a value of the nondimensional buckling force. In the case of axial compression, the nondimensional buckling force, $\mathscr{T}$, expresses the buckling load (P) related to the bending stiffness of the shell and the cylindrical shell radius:

$$\mathscr{T} = -P\frac{R}{2\pi\sqrt{D_{11}D_{22}}} \tag{84}$$

The prebuckling force component in the axial direction, $\overline{\mathscr{N}_{11}}$, as defined in Eq. (70), represents the nondimensional axial buckling force, $\mathscr{T}$, as shown in Eq. (84). If only an axial load is considered, and deeming the expression of the stress function as defined in Eqs. (71) and (72) the prebuckling force components $\overline{\mathscr{N}_{22}}$ and $\overline{\mathscr{N}_{12}}$ are equal to zero.

$$\overline{\mathscr{N}_{11}} = \frac{\partial^2 \overline{F}}{\partial z_2^2} = \mathscr{T} \tag{85}$$

$$\overline{\mathscr{N}_{22}} = \frac{\partial^2 \overline{F}}{\partial z_1^2} = \frac{\overline{\mathscr{N}_{12}}}{\alpha_b} = -\frac{\partial^2 \overline{F}}{\partial z_1 \partial z_2} = 0 \tag{86}$$

Compounding all the exposed derivations (Eqs. (74)–(76), (79)–(83), (85) and (86)) the following linearized buckling equations are obtained:

$$\alpha_b^2\frac{\partial^3 \widehat{B}_1}{\partial z_1^3} + \beta\frac{\partial^3 \widehat{B}_1}{\partial z_1 \partial z_2^2} + \frac{1}{\alpha_b^2}\frac{\partial^3 \widehat{B}_2}{\partial z_2^3} + \beta\frac{\partial^3 \widehat{B}_2}{\partial z_1^2 \partial z_2} = \mathscr{T}\frac{\partial^2 \widehat{W}}{\partial z_1^2} - \sqrt{12}Z\frac{\partial^2 \widehat{F}}{\partial z_1^2} \tag{87}$$

$$\alpha_m^2\frac{\partial^4 \widehat{F}}{\partial z_1^4} + \frac{1}{\alpha_m^2}\frac{\partial^4 \widehat{F}}{\partial z_2^4} + 2\mu\frac{\partial^4 \widehat{F}}{\partial z_1^2 \partial z_2^2} = \sqrt{12}Z\frac{\partial^2 \widehat{W}}{\partial z_1^2} \tag{88}$$

$$\chi_1 \widehat{B}_1 - \alpha_b^2\frac{\partial^2 \widehat{B}_1}{\partial z_1^2} + \frac{1}{2}(\beta - \nu_b)\frac{\partial^2 \widehat{B}_1}{\partial z_2^2} - \frac{1}{2}(\beta + \nu_b)\frac{\partial^2 \widehat{B}_2}{\partial z_1 \partial z_2} = \chi_1\frac{\partial \widehat{W}}{\partial z_1} \tag{89}$$

$$\chi_2 \widehat{B}_2 - \frac{1}{\alpha_b^2}\frac{\partial^2 \widehat{B}_2}{\partial z_2^2} + \frac{1}{2}(\beta - \nu_b)\frac{\partial^2 \widehat{B}_2}{\partial z_1^2} - \frac{1}{2}(\beta + \nu_b)\frac{\partial^2 \widehat{B}_1}{\partial z_1 \partial z_2} = \chi_2\frac{\partial \widehat{W}}{\partial z_2} \tag{90}$$

For simplicity, Eqs. (89) and (90) can be also expressed as follows:

$$\widehat{B}_1 - \frac{\alpha_b^2}{\chi_1}\frac{\partial^2 \widehat{B}_1}{\partial z_1^2} + \frac{1}{2\chi_1}(\beta - \nu_b)\frac{\partial^2 \widehat{B}_1}{\partial z_2^2} - \frac{1}{2\chi_1}(\beta + \nu_b)\frac{\partial^2 \widehat{B}_2}{\partial z_1 \partial z_2} = \frac{\partial \widehat{W}}{\partial z_1} \tag{91}$$

$$\widehat{B}_2 - \frac{1}{\chi_2 \alpha_b^2}\frac{\partial^2 \widehat{B}_2}{\partial z_2^2} + \frac{1}{2\chi_2}(\beta - \nu_b)\frac{\partial^2 \widehat{B}_2}{\partial z_1^2} - \frac{1}{2\chi_2}(\beta + \nu_b)\frac{\partial^2 \widehat{B}_1}{\partial z_1 \partial z_2} = \frac{\partial \widehat{W}}{\partial z_2} \tag{92}$$

Recalling that for simply supported boundary conditions: $\widehat{W} = \widehat{W}_{z_1 z_1} = 0$ at $z_1 = 0, 1$; then these equations admit separable solutions of the form:

$$\widehat{W} = A \sin(m\pi z_1)\sin(nz_2) \tag{93}$$

$$\widehat{F} = B \sin(m\pi z_1)\sin(nz_2) \tag{94}$$

$$\widehat{B}_1 = C \cos(m\pi z_1)\sin(nz_2) \tag{95}$$

$$\widehat{B}_2 = D \sin(m\pi z_1)\cos(nz_2) \tag{96}$$

The nondimensional buckling load ($\mathscr{T}$), which is the desired solution of the derived equations, is obtained solving the eigenvalue problem. The value is found for the combination of m and n coefficients that gives the lowest nondimensional buckling load value. These values represent the buckling mode of the shell. The value of m is associated with the number of halfwaves in the longitudinal direction, whereas the value of n is the value associated with the number of waves in the circumferential direction. In the case of an axisymmetric solution the value of n is equal to 1.

5. Linearized buckling equations neglecting transverse shear

Eqs. (87), (88), (91) and (92) are the linearized governing equations of the buckling of a sandwich shell that includes the transverse shear effects. To analyze the effect of the transverse shear, the equations without taking it into account are also considered. In this case, the transverse shear strains (ε_{xz}, ε_{yz} from Eqs. (10) and (11)), or as defined in their nondimensional form (Γ_{13}, Γ_{23} in Eqs. (17) and (18)), are negligible compared to other strain components, and therefore:

$$B_1 = \frac{\partial W}{\partial z_1} \tag{97}$$

$$B_2 = \frac{\partial W}{\partial z_2} \tag{98}$$

This consideration simplifies some of the equations and reduces the number of variables to only the nondimensional out-of-plane displacement, W and the nondimensional stress function, F. The constitutive equation (Eq. (54) becomes:

$$\begin{bmatrix} \mathscr{M}_{11} \\ \mathscr{M}_{22} \\ \mathscr{M}_{12} \end{bmatrix} = \begin{bmatrix} \alpha_b^2 & -\nu_b & 0 \\ -\nu_b & \frac{1}{\alpha_b^2} & 0 \\ 0 & 0 & \beta - \nu_b \end{bmatrix} \begin{bmatrix} \frac{\partial^2 W}{\partial z_1^2} \\ \frac{\partial^2 W}{\partial z_2^2} \\ \frac{\partial^2 W}{\partial z_1 \partial z_2} \end{bmatrix} \tag{99}$$

Therefore the equilibrium equation described in Eq. (73) becomes:

$$\begin{aligned} &\alpha_b^2 \frac{\partial^4 W}{\partial z_1^4} + 2\beta \frac{\partial^4 W}{\partial z_1^2 \partial z_2^2} + \frac{1}{\alpha_b^2}\frac{\partial^4 W}{\partial z_2^4} \\ &+ \frac{\partial^2 F}{\partial z_2^2}\frac{\partial^2 W}{\partial z_1^2} - 2\frac{\partial^2 F}{\partial z_1 \partial z_2}\frac{\partial^2 W}{\partial z_1 \partial z_2} + \frac{\partial^2 F}{\partial z_1^2}\left(\frac{\partial^2 W}{\partial z_2^2} - \sqrt{12}\,Z\right) = 0 \end{aligned} \tag{100}$$

The axial buckling load in this particular case is notated as P_0. The nondimensional buckling force without transverse shear, $\mathscr{T}_0$, is thus defined in analogous way as the buckling load with transverse shear, $\mathscr{T}$ (Eqs. (84) and (85)).

$$\overline{\mathscr{N}}_{11} = \frac{\partial^2 \overline{F}}{\partial z_2^2} = \mathscr{T}_0 = -P_0 \frac{R}{2\pi\sqrt{D_{11}D_{22}}} \tag{101}$$

The criterion is applied as described in Eqs. (80) and (81), where $\overline{W}$ and $\overline{F}$ represent the prebuckling solutions along the fundamental path and $\widehat{W}$, $\widehat{F}$ represent small perturbations at buckling. Considering that the initial prebuckling displacement, $\overline{W}$, is constant, the linearized buckling equations in this case become:

$$\alpha_b^2 \frac{\partial^4 \widehat{W}}{\partial z_1^4} + 2\beta \frac{\partial^4 \widehat{W}}{\partial z_1^2 \partial z_2^2} + \frac{1}{\alpha_b^2}\frac{\partial^4 \widehat{W}}{\partial z_2^4} = \mathscr{T}_0 \frac{\partial^2 \widehat{W}}{\partial z_1^2} - \sqrt{12}Z\frac{\partial^2 \widehat{F}}{\partial z_1^2} \tag{102}$$

$$\alpha_m^2 \frac{\partial^4 \widehat{F}}{\partial z_1^4} + \frac{1}{\alpha_m^2}\frac{\partial^4 \widehat{F}}{\partial z_2^4} + 2\mu \frac{\partial^4 \widehat{F}}{\partial z_1^2 \partial z_2^2} = \sqrt{12}Z\frac{\partial^2 \widehat{W}}{\partial z_1^2} \tag{103}$$

These linearized equations were also described by Nemeth and Schultz [5] as the linearized governing equations for laminate configurations, where $\mathscr{T}_0$ is the nondimensional buckling force as defined in Eq. (101). Assuming again simply supported boundary conditions ($\widehat{W} = \widehat{W}_{z_1 z_1} = 0$ at $z_1 = 0, 1$), and separable solutions defined in Eqs. (93) and (94), an eigenvalue problem can be solved to determine the nondimensional buckling load. The value is found for the combination of m and n coefficients that gives the lowest nondimensional buckling load value ($\mathscr{T}_0$). The values of m and n describe the buckling mode of the shell, since they represent the halfwaves in the longitudinal direction and the waves in the circumferential direction respectively.

Upon inspection of linearized equations with and without transverse shear, the influence of χ_1 and χ_2 is revealed as the main difference between them. In the case where these nondimensional parameters have large values, Eqs. (89) and (90) would become:

$$\widehat{B}_1 = \frac{\partial \widehat{W}}{\partial z_1} \tag{104}$$

$$\widehat{B}_2 = \frac{\partial \widehat{W}}{\partial z_2} \tag{105}$$

The remaining governing equations Eqs. (87) and (88) would be as represented in Eqs. (102) and (103).

The values of χ_1 and χ_2, as defined in Eqs. (61) and (62), represent the influence of the transverse shear effects of the core. In the cases where the values of χ_1 and χ_2 are large, it indicates that the core material is very stiff and thus the influence of the transverse shear effects is negligible. In this case, the value of the nondimensional buckling load, with ($\mathscr{T}$) and without ($\mathscr{T}_0$) transverse shear effects will be the same.

6. Applications

In this section, applications are discussed to illustrate the results derived from the presented nondimensional formulation and how the nondimensional parameters can be used to better understand sandwich composite buckling behavior. The goal of the nondimensional formulation and the applications shown in this section is threefold. First, it shows how cylindrical shells with different materials and dimensions share the same buckling behavior. Second, it demonstrates how to navigate the design space of sandwich composite shells and detect which parameters have a greater influence on the buckling response. Finally, it illustrates the cases with shell properties that require the inclusion of the transverse shear, and therefore the more complete formulation.

6.1. Influence of nondimensional parameters in the design space

In order to lay-out these goals, different shells are compared. The dimensions of the shells, as well as the facesheet laminate, core thickness and modulus are reported in Table 1. The facesheets are made of the same carbon fiber material, with the properties: $E_{11} = 150GPa$, $E_{22} =$

Table 1
Properties of the shells.

Properties	Shell 1	Shell 2	Shell 3	Shell 4	Shell 5	Shell 6
Radius, $R[mm]$	400	1400	400	400	400	400
Length, $L[mm]$	800	2800	800	800	800	1600
Faceheet laminate	$(\pm 45)_s$	$(\pm 45)_{s2}$	$(\pm 45)_s$	$(\pm 45)_s$	$(\pm 45)_s$	$(\pm 45)_s$
Core thickness, $t_{core}[mm]$	2.5	10	2.5	1	1	2.5
Core shear modulus, $G[MPa]$	120	70	364	120	70	120

$10GPa$, $G_{12} = 6GPa$, $\nu_{12} = 0.3$ and $t = 0.131mm$.

The nondimensional parameters (α_m, α_b, μ, β, ν_b, Z, χ_1 and φ) of the analyzed shells are reported in Table 2 together with the obtained nondimensional force with transverse shear ($\mathscr{F}$), without transverse shear ($\mathscr{F}_0$) and the ratio between them ($\mathscr{F}/\mathscr{F}_0$).

To demonstrate how nondimensional results are applicable to different shells of different scales, Shell 1 and Shell 2 are compared and their differences and similarities highlighted. Shell 2 is much larger than Shell 1, although in both cases the length is double the radius. The laminate of the facesheet of Shell 1 is $(\pm 45)_s$ (4 plies), whereas the laminate of the facesheet in Shell 2 is $(\pm 45)_{s2}$ (8 plies). The core material, isotropic in both shells, is Rohacell 200 for Shell 1 and Rohacell 110 for Shell 2. The relevant difference between these materials is the shear moduli, G, as shown in Table 1. The thickness of the core of the two shells is also different.

In spite of these shells being of different scales, the set of nondimensional parameters that rule the nondimensional linearized equations is the same, as shown in Table 2. As a result, both the nondimensional force with transverse shear ($\mathscr{F}$) and without transverse shear ($\mathscr{F}_0$) are the same in both shells. Therefore, the ratio between both nondimensional buckling forces $\mathscr{F}/\mathscr{F}_0 = 0.81$ is the same as well.

In order to examine how the change in the different parameters affects the relation $\mathscr{F}/\mathscr{F}_0$ and explain how to navigate the design space of sandwich composite shells with the help of nondimensional parameters, another shell is considered, named Shell 3 and described in Table 1. This shell has the same geometry (radius and length) as Shell 1. Shell 3 facesheets are made of the same carbon fiber material as Shell 1, layup is also $(\pm 45)_s$ and the core thickness is also $2.5mm$. The only difference between Shell 3 and Shell 1 is the type of core material, which in this case is Rohacell 300, an isotropic foam ($G = 370MPa$) that is stiffer than the foam used in Shell 1.

The set of nondimensional parameters for Shell 1 and Shell 3 is the same except for the value of χ_1. In order to analyze the differences and study the trends, it is plotted in Fig. 3 how the transverse shear buckling load ratio, $\mathscr{F}/\mathscr{F}_0$ is influenced by the nondimensional transverse shear χ_1 for the sandwich shell with the Batdorf-Stein parameter $Z = 50$. Fig. 3 and Table 2 show that higher values of nondimensional transverse shear χ_1 lead to higher agreement between a buckling load accounting for the transverse shear versus a buckling load that does not.

Table 2
Nondimensional parameters of the shells.

Parameter	Shell 1	Shell 2	Shell 3	Shell 4	Shell 5	Shell 6
α_m	0.5	0.5	0.5	0.5	0.5	0.25
α_b	0.5	0.5	0.5	0.5	0.5	0.25
μ	−0.5	−0.5	−0.5	−0.5	−0.5	−0.5
β	2.4	2.4	2.4	2.4	2.4	2.4
ν_b	0.75	0.75	0.75	0.75	0.75	0.75
Z	50	50	50	100	100	50
χ_1	500	500	1500	970	500	500
φ	4	4	4	4	4	16
$\mathscr{F}$	294	294	341	567	478	293
$\mathscr{F}_0$	361	361	366	692	692	359
$\mathscr{F}/\mathscr{F}_0$	0.81	0.81	0.93	0.82	0.69	0.81

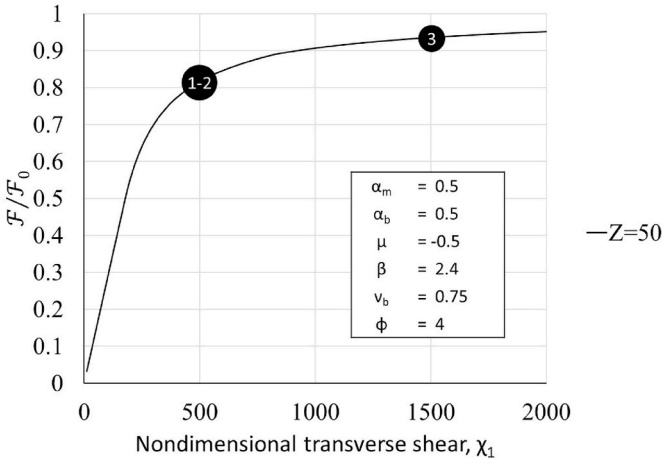

Fig. 3. Effect of core shear parameter (χ_1) on the transverse shear buckling load ratio ($\mathscr{F}/\mathscr{F}_0$) for $Z = 50$.

The curve in Fig. 3 is nonlinear and shows a steep increase for the values of χ_1 under 500. For the values over 500, the curve increase is more gradual. In the range depicted in Fig. 3, the curve also does not reach the value 1. This indicates that for this range of sandwich cylindrical shells, the transverse shear effects are not entirely negligible, inducing an error of at least 5% in the buckling load.

For the shells considered, as can be seen in Fig. 3, Shell 1 has a higher influence of the transverse shear in the solution ($\mathscr{F}/\mathscr{F}_0 = 0.81$) than Shell 3 ($\mathscr{F}/\mathscr{F}_0 = 0.93$). This is due to the fact that a stiffer core leads to a decrease in the influence of the transverse shear strains with respect to the rest of the strain components.

Shell 4 is now considered, where the geometry and facesheet laminate properties are the same as Shell 1 (See Table 1). Regarding the core, Shell 4 has the same material as Shell 1 ($G = 120MPa$), but the thickness of the core is reduced to only $1mm$. This case is a limit case because it goes close to infringing one of the assumptions of the methodology described in Section 2, that is, the core must be much thicker than the facesheet. In this case, the core is still double the thickness of the facesheet, so it is assumed that the method is still valid. Most nondimensional parameters remain the same as shown in Table 2, except the transverse shear parameter $\chi_1 = 1220$ and the Batdorf-Stein parameter $Z = 100$.

Fig. 4 shows for a sandwich shell with Batdorf-Stein parameters $Z =$

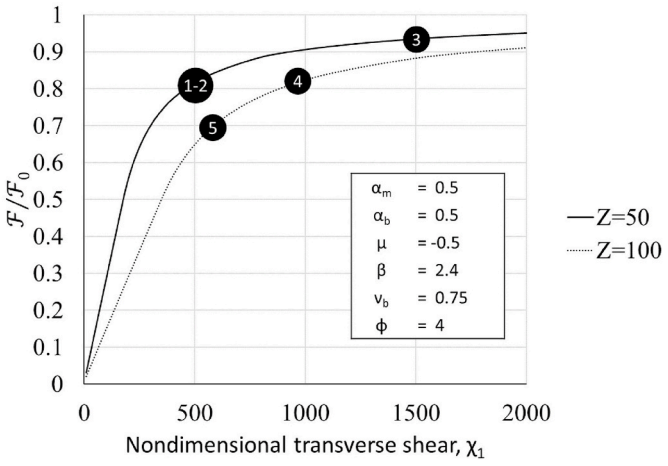

Fig. 4. Effect of core shear parameter (χ_1) on the transverse shear buckling load ratio ($\mathscr{F}/\mathscr{F}_0$) for $Z = 50$ and $Z = 100$.

50 and $Z = 100$, how the transverse shear buckling load ratio, $\mathscr{F}/\mathscr{F}_0$ is influenced by the nondimensional transverse shear χ_1. This is important because a variation in the shell that produces a change in the value of Z (i.e. core thickness) also produces a change in the value of χ_1. A change in core thickness from 2.5*mm* for Shell 1 to 1*mm* in Shell 4, changes both parameters χ_1 and Z so the influence is not easy to discern. In this particular scenario, the change in thickness does not produce a significant change in the influence of the transverse shear, going from $\mathscr{F}/\mathscr{F}_0 = 0.81$ for Shell 1 to $\mathscr{F}/\mathscr{F}_0 = 0.82$ for Shell 4.

Although the difference in the influence of the transverse shear remains similar, the buckling response of Shell 1 and Shell 4 is very different, as noted in the values of the nondimensional buckling load ranging from $\mathscr{F} = 294$ in Shell 1 to $\mathscr{F} = 567$ in Shell 4. Therefore the ratio $\mathscr{F}/\mathscr{F}_0$ is only an indication of the relevance of the transverse shear and not of the overall buckling response.

In Fig. 4, the influence of the transverse shear is higher for higher values of Z, which is a representative ratio of the radius versus the thickness. To observe this effect, Shell 5 is defined. The geometry and facesheet laminate properties of Shell 5 are the same as Shell 1 (See Table 1). Shell 5 has a core of a less stiff material ($G = 70MPa$) than Shell 1, and the thickness is reduced to only 1*mm*. Most nondimensional parameters remain the same, as shown in Table 2, except the Batdorf-Stein parameter $Z = 100$ and the transverse shear parameter $\chi_1 = 570$.

A higher value of Z with a similar value of χ_1, will have a more pronounced influence on the transverse shear. For instance, Shell 5 ratio is $\mathscr{F}/\mathscr{F}_0 = 0.69$, considerably lower than Shell 1 ratio $\mathscr{F}/\mathscr{F}_0 = 0.82$. The difference can also be spotted when comparing Shell 4 and Shell 5. Both shells have the same core thickness, and therefore the value of the nondimensional buckling load without transverse shear is the same ($\mathscr{F}_0 = 692$). However, when calculating the nondimensional buckling load including the transverse shear, for Shell 4 it is $\mathscr{F} = 567$ (18% lower than $\mathscr{F}_0$) and for Shell 5 it is $\mathscr{F} = 478$ (31% lower than $\mathscr{F}_0$). This is a remarkable disparity, considering that the shells core is made of similar material (isotropic foam) with only different shear moduli properties.

Finally, in order to study the influence of the length, Shell 6 is considered. Shell 6 has the same radius, facesheet laminate, core material and core thickness as Shell 1. However, the length of Shell 6 ($L = 1600mm$) is double the length of Shell 1 ($L = 800mm$). Therefore, Shell 1 and Shell 6 have different weighted geometry parameters (α_m, α_b) and different transverse ratio (φ). In order to study the effect of these parameters, it is plotted the transverse shear buckling load ratio, $\mathscr{F}/\mathscr{F}_0$ versus the weighted geometry parameters (α_m, α_b) for the sandwich shells with shear ratios $\varphi = 0.5$, $\varphi = 2$, $\varphi = 4$ and $\varphi = 16$ in Fig. 5.

If the same facesheet properties are kept, since the facesheet layup is $(\pm 45)_s$, the variation of α_m and α_b is dependent only in the variation of geometry ratio (L/R). Fig. 5 shows that low values of α_m and α_b, in combination with low values of φ can produce a big change in the transverse shear buckling load ratio, $\mathscr{F}/\mathscr{F}_0$. However, the change between Shell 1 and Shell 6 is not significant enough to change either the buckling behavior or the influence of the transverse shear $\mathscr{F}/\mathscr{F}_0 = 0.82$. For shells with moderate length with respect to the radius, the influence of α_m, α_b and φ does not play a significant role.

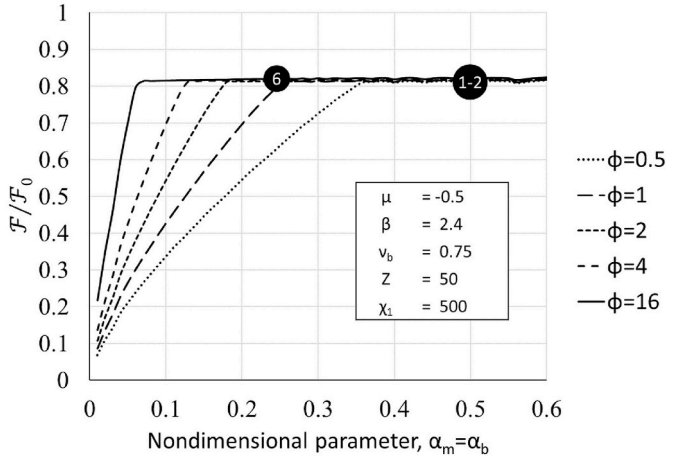

Fig. 5. Effect of weighted geometry parameters (α_m, α_b) on the transverse shear buckling load ratio ($\mathscr{F}/\mathscr{F}_0$) for $\varphi = 0.5$, $\varphi = 1$, $\varphi = 2$, $\varphi = 4$ and $\varphi = 16$.

6.2. Finite element verification

In order to verify the results and trends, for the shells described in Table 1 the buckling loads are compared with numerical results. The goal is to check the results obtained in Section 6.1, and analyze if the assumptions of the formulation hold even in the limit cases.

These numerical results are determined using the commercial general-purpose finite element code Abaqus, where a linear buckling analysis is performed. Since the considered sandwich cylindrical shells are assumed to be thin shells with thin cores, S4R reduced-integration four-noded shell elements are used in the finite element analysis. The models use elements of approximately 10 mm × 10 mm for Shell 1, 3, 4, 5 and 6 and 30 mm × 30 mm for Shell 2. Since the analytical equations are proposed considering simply supported conditions, simply supported conditions are used as well in the numerical analysis.

The results are reported in Table 3. The analytical load, P_0 is calculated using the formula in Eq. (101), and the analytical load, P is calculated using the formula in Eq. (84). The difference between the analytical load (P) and the numerical value (P_{num}) is also included in the table.

The numerical results show reasonable agreement(< 5%) with the analytical formulation for Shell 1, Shell 2, Shell 3 and Shell 6. For Shell 4, which is considered a limit case, results show a higher difference (−7.17%) between the analytical and the numerical result. The case is a limit case because the thickness of the core is comparable to the thickness of the facesheets. The assumption that the transverse shear is only carried by the core is no longer true. In this case, the transverse shear properties of the facesheets should also be taken into account and therefore the Cheung and Tennyson shear model used here [27] is no longer applicable. A large discrepancy can also be seen in Shell 5. For Shell 5, which has the same thickness (1*mm*) but a less stiff core material as Shell 4, results show that the analytical formulation overestimates the influence of the transverse shear by − 14.26%. This indicates that the reduction of the buckling load due to the transverse shear is significant ($P_{num}/P_0 = 0.81$) but not as high as predicted ($P/P_0 = 0.69$). This result reinforces the need to limit the application of the methodology to cases where the core thickness is significantly larger than the facesheets as established in the definition of the methodology.

Aside of the numerical buckling values, it is interesting to compare the buckling modes of the out-of-plane displacement w. The first comparison is between Shell 1 and Shell 2 which, as indicated, are shells of different scales, with different facesheet layup, core thickness and material. However, the nondimensional parameters that rule the buckling phenomena are the same and thus they have the same nondimensional buckling load ($\mathscr{F}$). The dimensional loads are different, as seen in Table 3, but they share the same eigenmode shape as seen in Fig. 6. The figure shows the first eigenmode shape for the out-of-plane displacement w.

Table 3
Buckling load of the shells.

Results	Shell 1	Shell 2	Shell 3	Shell 4	Shell 5	Shell 6
Analytical load, P_0 [*kN*]	657	4707	675	328	328	653
Analytical load, P[*kN*]	534	3826	630	269	227	533
Numerical load, P_{num}[*kN*]	551	3881	631	290	265	551
Analytical-numerical difference [%]	−3.02	−1.40	−0.18	−7.17	−14.26	−3.16

Regarding the comparison between shells of the same geometry (radius and length) it can be observed that they all have axisymmetric shape in Fig. 7. This is consistent with the eigenvalue solution obtained analytically as indicated in Eq. (93). Fig. 7 also shows the out-of plane displacement (w) for the first eigenmode. Each solution has a different number of half-waves: 11 for Shell 1, 10 for Shell 3, 14 for Shell 4 and 16 for Shell 5.

Finally, the buckling shapes of Shell 1 and Shell 6, for which the buckling load (P) as well as the buckling nondimensional load ($\mathscr{T}$) are very similar, are compared in Fig. 8. The buckling shape is axisymmetric in both cases but the number of half-waves is 11 for Shell 1 and 21 for Shell 2.

To finalize the verification process, it is worthy to mention that the model, as discussed in section 2, was not built to capture local buckling effects such as wrinkling. It was considered that the core normal stiffness was large enough so that the global modes occur at a much lower load. In order to assess the validity of this assumption, the wrinkling loads for described applications were calculated according the analytical formulation described in Ref. [30]:

$$P_{FW} = 4\pi R\, t_f \sqrt{\frac{2}{3}\frac{t_f}{t_c}\frac{E_c\sqrt{E_x E_y}}{1-\nu_{xy}\nu_{yx}}} \tag{106}$$

where R is the cylindrical shell midsurface radius, t_f is the facesheet thickness, t_c is the core thickness, E_c is the effective core extensional modulus, E_x and E_y are the effective facesheet extensional moduli in the axial and circumferential directions and ν_{xy} and ν_{yx} are the effective facesheet Poisson ratios. The results are reported in Table 4.

The comparison shows that the wrinkling load is higher than the expected buckling load and therefore the global buckling will occur before the local effects take place. Nevertheless, this is a conservative estimation applied to only a few cases. The framework could be extended to study the local effects such as wrinkling in the future.

7. Conclusions

This study presents the development of nondimensional equations for axial buckling of sandwich composite cylindrical shells with and without shear deformable core. A systematic nondimensionalisation is applied in order to obtain the nondimensional linearized buckling equations. The equations offer the advantage to present a similar format as their dimensional counterparts making their use more intuitive.

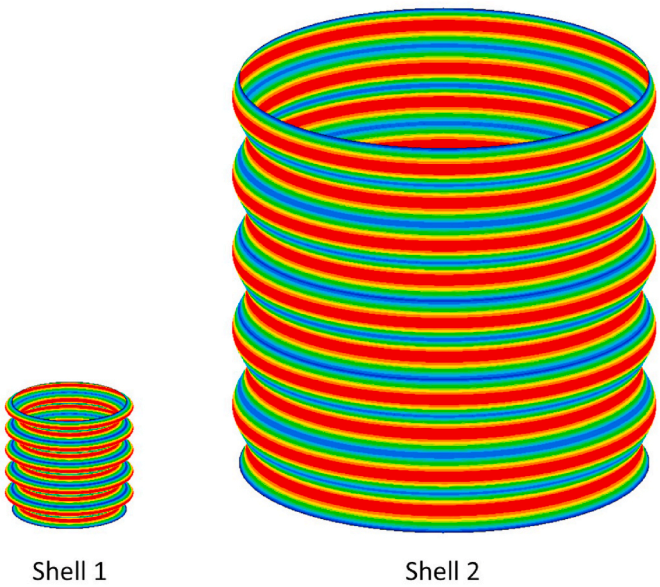

Fig. 6. Comparison of the first buckling mode of Shell 1 and Shell 2.

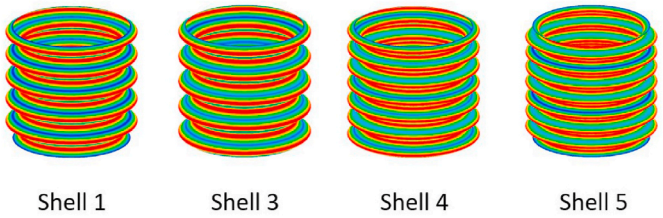

Fig. 7. Comparison of the first buckling mode of Shell 1, Shell 3, Shell 4 and Shell 5.

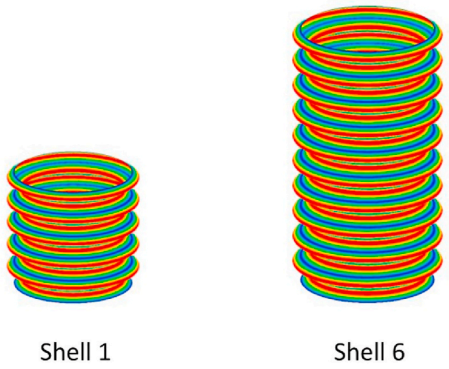

Fig. 8. Comparison of the first buckling mode of Shell 1 and Shell 6.

Table 4
Comparison of buckling and wrinkling loads.

Results	Shell 1	Shell 2	Shell 3	Shell 4	Shell 5	Shell 6
Global buckling load (analytical) $P[kN]$	534	3826	630	269	227	533
Wrinkling load (analytical) $P_{FW}[kN]$	14356	20727	7427	6467	5280	4102

A solution for the nondimensional buckling load is derived from the linearized nondimensional equations. The nondimensional buckling load is an effective parameter to compare the buckling phenomena for different types of shells of different scale. The nondimensional buckling load ($\mathscr{T}$) obtained considering the core transverse shear is compared to the nondimensional buckling load ($\mathscr{T}_0$) obtained neglecting the core transverse shear.

Using the nondimensional parameters, it is possible to navigate the design space of different shells and to investigate the impact of changes in the properties of the shells towards the buckling response. More specifically, the focus is in the reduction of the buckling load due to the influence of the core transverse shear effects and the relation between the load and other factors of the shells. The transverse shear buckling load ratio ($\mathscr{T}/\mathscr{T}_0$) represents this influence.

The study shows that the Batdorf-Stein parameter (Z) and the nondimensional transverse shear parameter (χ_1) influence the most the transverse shear buckling load ratio ($\mathscr{T}/\mathscr{T}_0$). Shells with a stiffer core material, represented with a higher nondimensional transverse shear parameter (χ_1), are less influenced by the core transverse shear. For the same value of χ_1, thinner shells, as represented by a higher Batdorf-Stein parameter (Z), present a higher transverse shear influence.

The study also investigates the influence of the shear modulus ratio (φ) and the weighted geometry nondimensional parameters (α_m, α_b) on the transverse shear buckling load ratio ($\mathscr{T}/\mathscr{T}_0$). In the applications considered (shells of moderate length with respect to the radius), the influence of these parameters is small.

Numerical values for specific examples are given. These examples

provide reasonable estimates to boundaries of the nondimensional design space for a range of cylindrical shells. For instance, in cases where the core is very thin compared to the facesheets and the material presents low shear stiffness, the formulation is shown to overstate the influence of the transverse shear and give conservative buckling load values.

Overall, the analysis and results can be used to design sandwich composite cylindrical shells. The nondimensionalisation is useful in order to compare shells of different sizes and analyze the influence of different parameters in the buckling response.

Declaration of competing interest

The authors declare that they have no known competing financial interests or personal relationships that could have appeared to influence the work reported in this paper.

Acknowledgments

The authors would like to thank Dr. Marc Schultz of NASA Langley Research Center who provided insight and expertise that greatly assisted the research. The discussions and constructive feedback on the topic vastly improved the work.

References

[1] M.P. Nemeth, Buckling of long compression-loaded anisotropic plates restrained against inplane lateral and shear deformations, Thin-Walled Struct. 42 (5) (2004) 639–685.
[2] I. Uriol Balbin, C. Bisagni, M.R. Schultz, M.W. Hilburger, Scaling methodology applied to buckling of sandwich composite cylindrical shells, AIAA J. (2020) 1–10.
[3] M. Hilburger, C. Rose, J. Starnes Jr., Nonlinear analysis and scaling laws for noncircular composite structures subjected to combined loads, in: 19th AIAA Applied Aerodynamics Conference, no. 1335, 2001.
[4] S. Batdorf, A simplified method of elastic-stability analysis for thin cylindrical shells, Tech. Rep. NASA TP 874 (1947).
[5] M. Nemeth, Nondimensional parameters and equations for nonlinear and bifurcation analyses of thin anisotropic quasi-shallow shells, Tech. Rep. NASA TP (2010) 216726.
[6] P. Weaver, J. Driesen, P. Roberts, Anisotropic effects in the compression buckling of laminated composite cylindrical shells, Compos. Sci. Technol. 62 (1) (2002) 91–105.
[7] I. Yang, C. Liu, Buckling and bending behaviour of initially stressed specially orthotropic thick plates, Int. J. Mech. Sci. 29 (12) (1987) 779–791.
[8] H. Wagner, C. Hühne, S. Niemann, R. Khakimova, Robust design criterion for axially loaded cylindrical shells-simulation and validation, Thin-Walled Struct. 115 (2017) 154–162.
[9] H. Wagner, E. Petersen, R. Khakimova, C. Hühne, Buckling analysis of an imperfection-insensitive hybrid composite cylinder under axial compression–numerical simulation, destructive and non-destructive experimental testing, Compos. Struct. 225 (2019), 111152.
[10] P. Seide, V. Weingarten, J. Petersen, NASA/SP-8007, Buckling of Thin-Walled Circular Cylinders, Nasa Space Vehicle Design Criteria (Structures), 1965.
[11] M.R. Schultz, D.W. Sleight, N.W. Gardner, M.T. Rudd, M.W. Hilburger, T. Palm, N. J. Oldfield, Test and analysis of a buckling-critical large-scale sandwich composite cylinder, in: 2018 AIAA/ASCE/AHS/ASC Structures, Structural Dynamics, and Materials Conference, no. 1693, 2018.
[12] C. Bisagni, Buckling tests of sandwich cylindrical shells with and without cut-outs, in: American Society for Composites 31st Technical Conference and ASTM Committee D30 Meeting, 2016, pp. 1–10.
[13] C. Alain, R. Ute, Pitfalls in the finite element modeling of the buckling of sandwich shells of revolution, Thin-Walled Struct. 63 (2013) 91–97.
[14] M. Alfano, C. Bisagni, Probability-based methodology for buckling investigation of sandwich composite shells with and without cut-outs, Int. J. Comput. Methods Eng. Sci. Mech. 18 (1) (2017) 77–90.
[15] E. Ghazali, M.L. Dano, A. Gakwaya, C.O. Amyot, Experimental and numerical studies of stepped-scarf circular repairs in composite sandwich panels, Int. J. Adhesion Adhes. 82 (2018) 41–49.
[16] M. Alfano, C. Bisagni, Probabilistic buckling analysis of composite and sandwich cylindrical shells, in: 55th AIAA/ASMe/ASCE/AHS/SC Structures, Structural Dynamics, and Materials Conference, 2014, 0166.
[17] M.W. Hilburger, J.H. Starnes Jr., Effects of imperfections of the buckling response of composite shells, Thin-Walled Struct. 42 (3) (2004) 369–397.
[18] L. Friedrich, S. Loosen, K. Liang, M. Ruess, C. Bisagni, K.U. Schröder, Stacking sequence influence on imperfection sensitivity of cylindrical composite shells under axial compression, Compos. Struct. 134 (2015) 750–761.
[19] M.F. Caliri Jr., A.J. Ferreira, V. Tita, A review on plate and shell theories for laminated and sandwich structures highlighting the finite element method, Compos. Struct. 156 (2016) 63–77.
[20] A. Noor, W. Burton, Assessment of shear deformation theories for multilayered composite plates, Appl. Mech. Rev. 42 (1) (1989) 1–13.
[21] A. Pirrera, P.M. Weaver, Geometrically nonlinear first-order shear deformation theory for general anisotropic shells, AIAA J. 47 (3) (2009) 767–782.
[22] K.H. Lo, R.M. Christensen, E.M. Wu, A high-order theory of plate deformation - Part 2: laminated plates, J. Appl. Mech. 44 (4) (1977) 669–676.
[23] E. Viola, F. Tornabene, N. Fantuzzi, General higher-order shear deformation theories for the free vibration analysis of completely doubly-curved laminated shells and panels, Compos. Struct. 95 (2013) 639–666.
[24] M. Cho, K.-O. Kim, M.-H. Kim, Efficient higher-order shell theory for laminated composites, Compos. Struct. 34 (2) (1996) 197–212.
[25] A. Gorgeri, R. Vescovini, L. Dozio, Analysis of Multiple-Core Sandwich Cylindrical Shells Using a Sublaminate Formulation, Composite Structures, 2019, p. 111067.
[26] M. Nemeth, Nondimensional parameters and equations for buckling of anisotropic shallow shells, J. Appl. Mech. 61 (3) (1994) 664–669.
[27] E. Cheung, R.C. Tennyson, Buckling of composite sandwich cylinders under axial compression, in: Studies in Applied Mechanics, vol. 19, Elsevier, 1988, pp. 151–181.
[28] J. Arbocz, C. Bisagni, A. Calvi, E. Carrera, R. Cuntze, R. Degenhardt, N. Gualtieri, H. Haller, N. Impollonia, M. Jacquesson, E. Jansen, H.-R. Meyer-Piening, H. Oery, A. Rittweger, R. Rolfes, G. Schullerer, G. Turzo, T. Weller, J. Wijker, Space Engineering - Buckling of Structures ECSS-E-HB-32-24a, 2010.
[29] J. Singer, J. Arbocz, T. Weller, Buckling Experiments, Basic Concepts, Columns, Beams and Plates, vol. 1, John Wiley & Sons, 1998.
[30] J.R. Vinson, The Behavior of Sandwich Structures of Isotropic and Composite Materials, CRC Press, 1999.